Numerical method for solving stochastic differential equations with dichotomous noise

Changho Kim and Eok Kyun Lee
Department of Chemistry and School of Molecular Science (BK21), Korea Advanced Institute of Science and Technology, Daejeon 305-701, Republic of Korea

Peter Talkner
Institut für Physik, Universität Augsburg, D-86135 Augsburg, Germany
(Received 18 October 2005; published 1 February 2006)

We propose a numerical method for solving stochastic differential equations with dichotomous Markov noise. The numerical scheme is formulated such that (i) the stochastic formula used follows the Stratonovich-Taylor form over the entire range of noise correlation times, including the Gaussian white noise limit; and (ii) the method is readily applicable to dynamical systems driven by arbitrary types of noise, provided there exists a way to describe the random increment of the stochastic process expressed in the Stratonovich-Taylor form. We further propose a simplified Taylor scheme that significantly reduces the computation time, while still satisfying the moment properties up to the required order. The accuracies and efficiencies of the proposed algorithms are validated by applying the schemes to two prototypical model systems that possess analytical solutions.

DOI: 10.1103/PhysRevE.73.026101 PACS number(s): 02.50.Ey, 02.60.Cb, 05.40.Ca

I. INTRODUCTION

The concept of stochastic dynamics has provided a new paradigm for diverse areas of science, engineering, and finance. Stochastic formulations take into account the inherent fluctuations of the embedded system, which play a key role in describing characteristic features of the dynamical process. These theories have found a wide range of applications in the physical sciences, including dynamical systems far from equilibrium.

Two approaches have been developed for studying stochastic processes in systems subject to noise. The first approach is based on a stochastic differential equation that describes the evolution of stochastic processes through the realization of noise. As in the case of ordinary differential equations, analytical solutions of stochastic differential equations are available only for very limited cases—linear systems or nonlinear systems reducible to linear forms by appropriate transformation techniques [1,2]. On the other hand, numerical schemes based on discrete time approximations are available for various types of nonlinear stochastic differential equations. The second approach is to analytically or numerically solve the Fokker-Planck equation [3,4] describing the evolution of the corresponding probability density function. However, their applicability is restricted to processes driven by Gaussian white noise [5], and numerical solution of the Fokker-Planck equation quickly becomes expensive even for systems with only a modest number of degrees of freedom. In the case of processes driven by colored noise such as Ornstein-Uhlenbeck or dichotomous Markov noise the corresponding master equation describing the evolution of the probability density function becomes a rather intractable integro-differential equation with respect to time and space [6–8].

Both of the approaches currently available have their share of advantages and disadvantages. From a numerical viewpoint, however, stochastic differential equations are easier to solve than the Fokker-Planck equation. In practice, the advent of modern supercomputers has made it possible to run a large number of path realizations of stochastic differential equations. Each sample trajectory, consistent with a given stochastic equation, is generated by the Monte Carlo technique, and the statistical properties of interest are obtained by taking averages over many of these simulated trajectories. This procedure is simpler and often much faster than solving the partial differential equations of the Fokker-Planck equation. Furthermore, this method can be applied to various forms of stochastic equations, including systems with several variables.

The main shortcoming of the stochastic equation approach is that a large number of sample paths must be simulated to generate statistically reliable results. The statistical error due to finite sampling is proportional to $1/\sqrt{N}$, where N is the number of sample paths. Another type of error, called the systematic error, arises from the finite size of the time step. The use of a smaller time step, though, not only increases the computation time required to generate each sample trajectory, but also requires a larger number of sample trajectories to obtain statistically more reliable results. Hence a compromise must be made between accuracy and computational cost. However, computation cost is becoming less of an impediment due to continuing increases in computing power and the adoption of parallel computing, as well as the development of more efficient numerical integration schemes and variance reduction methods.

A great variety of numerical algorithms have been developed to solve stochastic differential equations subject to Gaussian white noise [1,9,10], all of which use a stochastic Taylor expansion technique based on a discrete time approximation. Depending on the quality of the discrete time approximation, the methods are classified as strong or weak schemes. Methods that generate good approximations of individual paths are considered strong schemes, whereas those

that generate only a probability distribution and its moment are considered weak schemes.

The methods developed to solve stochastic differential equations subject to Gaussian white noise can be extended in a straightforward manner to systems driven by exponentially correlated colored Gaussian noise (the Ornstein-Uhlenbeck process). Since the Ornstein-Uhlenbeck process is generated by a linear stochastic differential equation subject to Gaussian white noise, the stochastic equation for the system variable can be solved numerically along with this auxiliary equation.

However, as Mannella [10] argued, such methods do not give satisfactory results for some cases. A stiff problem owing to very different time scales can occur when the correlation time of the noise approaches zero. Different algorithms which are implicit for the noise [11,12] have been developed by taking advantage of the fact that the auxiliary equation describing the Ornstein-Uhlenbeck process is linear so that this process can be integrated analytically. This approach works for any length of the correlation time of the noise, while the integration time step is kept constant. No downgrading in the convergence is found, and no problems related to stiffness of the system are expected.

Along with the Ornstein-Uhlenbeck process, the dichotomous Markov process (also known as the random telegraph signal) is another important type of colored noise that has applications in various fields of science. In addition to mimicking the effects of the finite correlation time of the real noise, the dichotomous Markov process may directly provide a realistic representation of an actual physical situation (e.g., thermal transitions between two configurations or states). The stationary probability density of an arbitrary single-variable system driven by dichotomous noise with finite correlation time has been obtained analytically. In addition, the dynamics of the transitions induced by this noise and the effect of the correlation time of the noise on the dynamical system have been extensively studied [13–17]. Dynamical features of processes driven by dichotomous noise usually are not available by analytical means. As stated above, the time-dependent probability density satisfies, in general, a rather intractable integro-differential equation in time. This equation can be reduced to a differential equation of finite order only in very rare cases where specific conditions are satisfied [8]. As a result, analytical solutions are available for only a few cases [18], and even in those cases, the solutions are remarkably complicated and contain δ functions at the boundaries. Moreover, we would note that most of the analytical features of the dynamics driven by dichotomous Markov noise are limited to systems with a single scalar variable [19,20].

In this paper, we present a numerical method for simulating a stochastic dynamical system subject to dichotomous noise. This method enables the generation of sample trajectories under uniform time discretization regardless of the correlation length of the noise. The mathematical formalism of our scheme reduces to the Euler form as the correlation time of the dichotomous noise goes to zero.

The remainder of this paper is organized as follows. In Sec. II, some properties of dichotomous noise and previous numerical methods are presented. In Sec. III, the formulations of the stochastic integration scheme and its simplified version are presented. In Sec. IV, numerical tests are presented in which our methods are applied to two typical cases for which analytical solutions are known. Finally, we present our conclusions in Sec. V.

II. THEORETICAL BACKGROUND

We consider a stochastic process described by a nonlinear stochastic dynamical system driven by dichotomous Markov noise,

$$\dot{x}(t) = f(x(t)) + g(x(t))\xi(t), \tag{1}$$

where f and g are nonlinear functions of x, and $\xi(t)$ is a symmetric dichotomous noise which switches back and forth between two values $\pm a$ with transition rate λ. We assume $\xi(t)$ is a stationary process. Then the mean and the autocorrelation of $\xi(t)$ can be expressed as follows:

$$\langle \xi(t) \rangle = 0, \tag{2}$$

$$\langle \xi(t)\xi(t') \rangle = a^2 \exp(-2\lambda|t-t'|). \tag{3}$$

We note that by taking $\lambda \to \infty$ and $a \to \infty$ with $a^2/\lambda = 2D$ fixed, the white noise limit property is recovered:

$$\langle \xi(t)\xi(t') \rangle = 2D\delta(t-t'). \tag{4}$$

The sojourn times for staying in the $+a$ or $-a$ state without flipping are governed by the following exponential distribution:

$$\Psi(s) = \lambda e^{-\lambda s}. \tag{5}$$

The probabilities $P_{\pm}(\tau)$ that $\xi(\tau) = \pm a$ satisfy the following master equation:

$$\frac{d}{d\tau}\begin{bmatrix} P_+(\tau) \\ P_-(\tau) \end{bmatrix} = \begin{bmatrix} -\lambda & \lambda \\ \lambda & -\lambda \end{bmatrix}\begin{bmatrix} P_+(\tau) \\ P_-(\tau) \end{bmatrix}. \tag{6}$$

If the initial condition is given by $P_+(0) = 1$ and $P_-(0) = 0$, the solution for Eq. (6) is

$$P_{\pm}(\tau) = \frac{1}{2}(1 \pm e^{-2\lambda\tau}). \tag{7}$$

Notice that $P_+(\tau)$ in Eq. (7) denotes the probability that the noise, which was initially in the $+a$ (or $-a$) state, returns to the same state after time τ, and $P_-(\tau)$ denotes the probability that the noise state at time τ differs from the initial state, regardless of the noise states between time 0 and τ. Then, one straightforward way to generate $\xi(t)$ would be as follows:

$$\xi(\Delta t) = \begin{cases} \xi(0) & \text{w.p. } P_+(\Delta t), \\ -\xi(0) & \text{w.p. } P_-(\Delta t), \end{cases} \tag{8}$$

where w.p. is an abbreviation of "with probability." First, we generate a uniform random number U on (0, 1) and then compare the magnitude of U with $P_+(\Delta t)$. If $U < P_+(\Delta t)$, we set $\xi(\Delta t) = \xi(0)$, and otherwise, $\xi(\Delta t) = -\xi(0)$. Having obtained $\xi(t)$ in this way, we can then perform a numerical

integration using the following approximate form of Eq. (1) (we shall refer to this as method 1):

$$x(\Delta t) \approx x(0) + [f(x(0)) + g(x(0))\xi(0)]\Delta t. \tag{9}$$

This approximation corresponds to the lowest order Taylor expansion if $\xi(t)$ is a deterministic smooth function of time. This scheme works well provided λ is sufficiently small that $\xi(t)$ is unlikely to change its value during Δt. However, as λ becomes larger, $\xi(t)$ can vary during Δt, and the approximation imposed in Eq. (9) becomes inappropriate. Moreover, this approach does not allow systematic improvement of the formalism to a higher order approximation while maintaining the stochastic nature of $\xi(t)$.

The problem inherent in method 1 can be remedied in a simple manner. Equation (5) enables one to generate sample trajectories as proposed by Palleschi [21]. The sojourn time s_i obeying the exponential distribution $\Psi(s)$ is sampled from

$$s_i = -\frac{1}{\lambda}\ln(1 - U_i) \tag{10}$$

where U_i is a random number that is uniformly distributed on the unit interval. Since $\xi(t)$ has a constant value of $+a$ (or $-a$) from t_i to $t_{i+1}=t_i+s_i$, Eq. (1) is reduced to the ordinary differential equation $\dot{x}=f_+(t)$ [or $\dot{x}=f_-(t)$ depending on the value of $\xi(t)$ during that period], where $f_\pm(x)=f(x)\pm ag(x)$. This means that for each time interval $[t_i, t_{i+1}]$, this equation can be solved using standard numerical methods for integrating ordinary differential equations. (We shall refer to this as method 2.) Although numerical simulation following this procedure can be effective owing to the simple structure of dichotomous noise, this method causes serious problems when applied to stiff systems in which the noise has a short correlation time. In this region, most of the sojourn times s_i become so small that the computation time increases sharply. In addition, the round-off error increases as the integration of $\dot{x}$ proceeds.

Two limiting behaviors are possible for stiff systems: (1) the well known Gaussian white noise limit, which is described above; and (2) the white shot noise limit, which can be thought of as a sequence of δ peaks at random points in time. White shot noise can be obtained from the asymmetric dichotomous noise, which takes values a_+ and a_- and leaves these states with rates λ_+ and λ_-, respectively. With this type of asymmetric dichotomous noise, white shot noise is obtained by taking $\lambda_+ \to \infty$ and $a_+ \to \infty$ with a_+/λ_+ fixed [22].

The two above mentioned numerical methods (methods 1 and 2) are unable to show correct limiting behavior for either Gaussian white noise or white shot noise. Furthermore, systematic error analysis and study of the effect of the correlation time of the noise for arbitrary values of λ are rather difficult under these schemes. Figure 1 shows the stationary distribution of x obtained using three numerical methods (methods 1 and 2, and our formalism, method A, which is presented in the next section) along with the analytical result for a simple case $f(x)=-x$ and $g(x)=1$. The parameter values used in this computation were $\lambda=10$ and $D=a^2/2\lambda=1$. The integration time step Δt was set to 0.01 in the calculations of the trajectories using methods 1 and A. In the case of method 2, for each s_i obtained from Eq. (10), s_i was divided into n equal subintervals (where n is chosen such that the length of the subinterval is as close as possible to $\Delta t=0.01$), and numerical integrations were performed using the standard Euler method. To obtain a stationary state, data were gathered after an equilibration time, where $t=10$ time units was usually sufficient for equilibration. After the equilibration, each trajectory was saved at intervals of $10\Delta t$ until 100 points were collected. A total of 10^4 sample trajectories were generated, and the stationary probability density was obtained from the data collected from those sample trajectories. The distribution obtained by method 1 differs markedly from the analytical result, whereas the results obtained using methods A and 2 are almost indistinguishable from the analytical result.

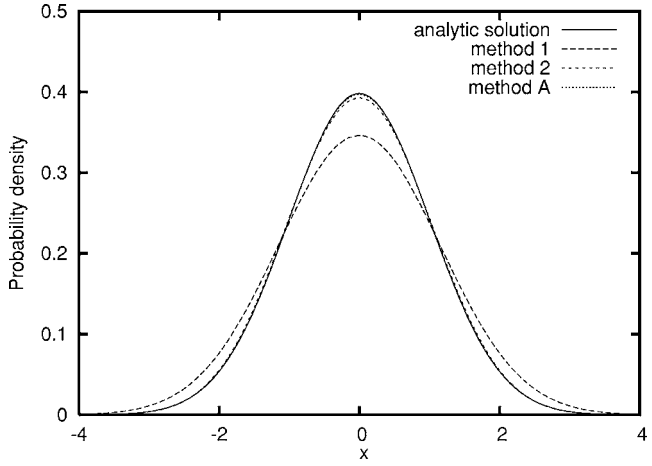

FIG. 1. Comparison of the stationary probability distributions obtained using three numerical methods (methods 1, 2, and A) along with the analytical result for a simple case $f(x)=-x$ and $g(x)=1$.

The numerical method we propose in this paper starts with the following standard form of the stochastic Taylor expansion:

$$x(\Delta t) \approx x(0) + f(x(0))\Delta t + g(x(0))\Delta X \tag{11}$$

where ΔX is the random increment defined as

$$\Delta X = \int_0^{\Delta t} \xi(u)du. \tag{12}$$

If $\xi(t)$ is Gaussian white noise, the stochastic time discretization formula shown in Eq. (11) is reduced to the Euler scheme. In this case, the stochastic integral ΔX itself is a Wiener process that is Gaussian as well as Markovian. On the other hand, if $\xi(t)$ is dichotomous noise with finite correlation time, ΔX is no longer either Gaussian or Markovian. However, the two-dimensional process described by ΔX along with the state of $\xi(t)$ is Markovian, and this property enables us to develop a numerical simulation scheme to solve more general forms of stochastic differential equations with non-Markovian noise.

III. NUMERICAL SIMULATION SCHEME FOR A STOCHASTIC DYNAMICAL SYSTEM

A. Stochastic integration under the discrete time approximation

Integrating Eq. (1) with initial condition $x(0)=x_0$, we may write

$$x(\Delta t) = x_0 + \int_0^{\Delta t} f_u du + \int_0^{\Delta t} g_u \xi(u) du \tag{13}$$

where we have used the simplified notation $h_u = h(x(u))$. Note that, in the present paper, the subscript u designates the evaluation of a given functional at time u, not partial differentiation with respect to u. (For differentiation, we use the notation h'.) Equation (13) is merely a formal solution. Applying the chain rule, which can be written as

$$h_t = h_0 + \int_0^t h'_u [f_u + g_u \xi(u)] du, \tag{14}$$

Eq. (13) can be transformed to

$$x(\Delta t) = x_0 + f_0 \int_0^{\Delta t} du + g_0 \int_0^{\Delta t} \xi(u) du + R_1 \tag{15}$$

where

$$R_1 = \int_0^{\Delta t} \int_0^u f'_w [f_w + g_w \xi(w)] dw\, du + \int_0^{\Delta t} \int_0^u g'_w [f_w + g_w \xi(w)] dw\, \xi(u) du. \tag{16}$$

Applying Eq. (14) to R_1, we obtain

$$R_1 = f'_0 f_0 \int_0^{\Delta t} \int_0^u dw\, du + f'_0 g_0 \int_0^{\Delta t} \int_0^u \xi(w) dw\, du + g'_0 f_0 \int_0^{\Delta t} \int_0^u dw \xi(u) du + g'_0 g_0 \int_0^{\Delta t} \int_0^u \xi(w) dw \xi(u) du + R_2 \tag{17}$$

where R_2 is the remainder consisting of triple integral terms. Note that the integrands in Eq. (17) depend on the trajectory of the noise only, contrary to those in Eq. (16). We can continue with successive substitutions and obtain a higher order approximation with the remainder R_n. The stochastic Taylor expansion obtained in this way follows the Stratonovich-Taylor expansion form [1]. Our expansion follows the Stratonovich-Taylor expansion form rather than the Ito-Taylor expansion form because the Stratonovich calculus obeys the ordinary rules of calculus such as the chain rule shown in Eq. (14). Therefore, in the white noise limit, the set of solutions of the differential equation (1) tends to the set of solutions obtained by applying the Stratonovich integration rule [3,23].

Since symmetric dichotomous noise has the special property that $|\xi(t)| = a$, the order of magnitude of each expansion term with respect to Δt can be easily estimated. For some constant M, we have

$$\left| \int_0^{\Delta t} h_u \xi(u) du \right| \leq a \int_0^{\Delta t} |h_u| du \leq M \Delta t. \tag{18}$$

In a similar way, the order of magnitude of R_1 and R_2 can be estimated as $O(\Delta t^2)$ and $O(\Delta t^3)$, respectively. In general, the order of magnitude of R_n is estimated as $O(\Delta t^{n+1})$. Therefore Eq. (11) [the same as Eq. (15)] is exact up to first order with respect to Δt and truncation at R_n yields a solution that is exact up to nth order.

Let us consider the following form of the approximation:

$$x(\Delta t) \approx x_0 + f_0 \Delta t + g_0 \Delta X + \frac{1}{2} g'_0 g_0 \Delta X^2, \tag{19}$$

where the random increment ΔX is defined in Eq. (12). Compared with the first order form defined in Eq. (11), Eq. (19) has an additional term that is obtained from the last double integral on the right hand side of Eq. (17), since

$$\int_0^{\Delta t} \int_0^s \xi(u) du \xi(s) ds = \frac{1}{2} \left(\int_0^{\Delta t} \xi(s) ds \right)^2. \tag{20}$$

This term is second order with respect to Δt. In the white noise limit, however, this term becomes first order because ΔX tends to a Wiener process (of order $\Delta t^{1/2}$). In this limit, the stochastic expansion in Eq. (19) becomes identical to the first order algorithm [11] employed for the system driven by Gaussian white noise. Therefore, by including this term, the accuracy of Eq. (19) can be maintained even in the vicinity of the white noise limit. A similar algorithm has been proposed by Sancho *et al.* for systems driven by an Ornstein-Uhlenbeck process [11].

Next, we would like to know the distribution of the random increment ΔX. To be more precise, since the distribution of ΔX depends on the state of $\xi(0)$ and $\xi(\Delta t)$, what we actually wish to know is the conditional probability $p(\Delta X = z \,|\, \xi(0), \xi(\Delta t))$. We consider the following process:

$$X(\tau) = \int_0^\tau \xi(u) du. \tag{21}$$

Then a Markov process results for the two-dimensional process described by $(\xi(\tau), X(\tau))$. Hence the following master equation describes the space-time-dependent behavior of the probability distribution of the extended Markov process $(\xi(\tau), X(\tau))$:

$$\frac{\partial}{\partial \tau} p_+(z,\tau) = -a \frac{\partial}{\partial z} p_+ - \lambda p_+ + \lambda p_-,$$

$$\frac{\partial}{\partial \tau} p_-(z,\tau) = a \frac{\partial}{\partial z} p_- - \lambda p_- + \lambda p_+, \tag{22}$$

where $p_\pm(z,\tau)$ are the probability densities that $X(\tau)=z$ and $\xi(\tau)=\pm a$, respectively.

In the present case, we consider the following two initial conditions for $p_\pm(z,\tau)$ at $\tau=0$:

$$p_+(z,0) = \delta(z) \text{ and } p_-(z,0) = 0, \tag{23}$$

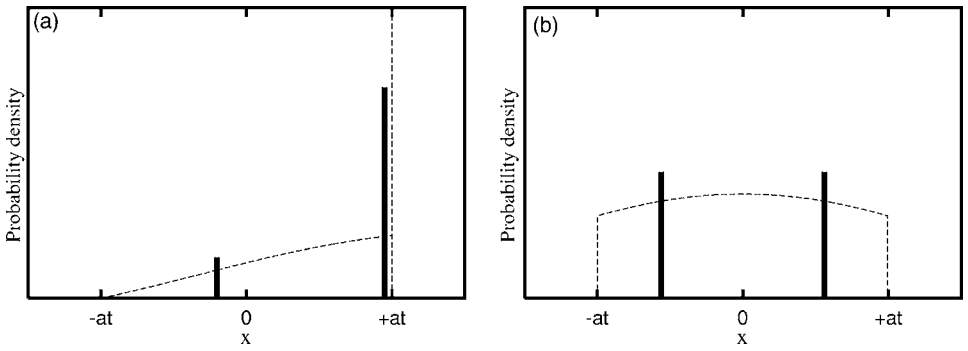

FIG. 2. Probability distributions of ΔX_i and $\Delta \tilde{X}_i$: $i=$(a) 1 and (b) 2. The dashed lines represent the probability distributions $p_i(z|\Delta t)$ in Eq. (34), and the solid bars represent the positions of two possible values of $\Delta \tilde{X}_i$ [R_i and L_i in Eq. (38)] with the probabilities q_i and $1-q_i$, respectively, which are proportional to the heights.

$$p_+(z,0)=0 \text{ and } p_-(z,0)=\delta(z). \tag{24}$$

Since the initial condition (23) means that $\xi(0)=+a$, from the solution of Eq. (22) we can obtain both $p(\Delta X=z|\xi(0)=+a,\xi(\Delta t)=+a)$ and $p(\Delta X=z|\xi(0)=+a,\xi(\Delta t)=-a)$. Likewise, from the solution $p_\pm(z,\Delta t)$ for the initial condition (24), we can calculate both $p(\Delta X=z|\xi(0)=-a,\xi(\Delta t)=+a)$ and $p(\Delta X=z|\xi(0)=-a,\xi(\Delta t)=-a)$. This means that we have to know the behavior of individual probability densities $p_+(z,\tau)$ and $p_-(z,\tau)$ separately, rather than the total probability density $p(z,\tau)=p_+(z,\tau)+p_-(z,\tau)$ [18,24,25]. The symmetric structure of Eq. (22) implies that the solution $p_\pm(z,\tau)$ has the following symmetry property depending on the initial condition. If we write the solution of Eq. (22) as $\tilde{p}_+(z,\tau)$ and $\tilde{p}_-(z,\tau)$ with the initial condition (23), the solutions with the initial condition (24) are $\tilde{p}_-(-z,\tau)$ and $\tilde{p}_+(-z,\tau)$. Therefore it is sufficient to solve Eq. (22) with the initial condition (23) only.

The procedure to analytically solve Eq. (22) starts with the transformation of Eq. (22) to the following single second order differential equation which has both $p_+(z,\tau)$ and $p_-(z,\tau)$ as solutions [24]:

$$\left(\frac{\partial^2}{\partial\tau^2}+2\lambda\frac{\partial}{\partial\tau}-a^2\frac{\partial^2}{\partial z^2}\right)p_\pm(z,\tau)=0. \tag{25}$$

Let us replace z and τ by the new independent variables ϕ and ψ, which are known as characteristics,

$$\phi=z+a\tau,$$

$$\psi=z-a\tau. \tag{26}$$

Then, by change of variables, Eq. (25), which is in the form of a hyperbolic partial differential equation, is reduced to the following canonical form:

$$\left(\frac{\partial^2}{\partial\phi\,\partial\psi}-\frac{\lambda}{2a}\frac{\partial}{\partial\phi}+\frac{\lambda}{2a}\frac{\partial}{\partial\psi}\right)p_\pm(\phi,\psi)=0. \tag{27}$$

Since ϕ and ψ coincide for $\tau=0$, boundary conditions of $p_\pm(\phi,\psi)$ in Eq. (27) are obtained from each initial condition shown in (23) and (24), as follows:

$$p_+(\phi,\psi)|_{\phi=\psi}=\delta(\phi),$$

$$\left(\frac{\partial}{\partial\phi}-\frac{\partial}{\partial\psi}\right)p_+(\phi,\psi)\bigg|_{\phi=\psi}=-\delta'(\phi)-\frac{\lambda}{a}\delta(\phi), \tag{28}$$

$$p_-(\phi,\psi)|_{\phi=\psi}=0,$$

$$\left(\frac{\partial}{\partial\phi}-\frac{\partial}{\partial\psi}\right)p_-(\phi,\psi)\bigg|_{\phi=\psi}=\frac{\lambda}{a}\delta(\phi). \tag{29}$$

The Cauchy problem of finding the solution of Eq. (27) that satisfies initial condition (28) or (29) can be solved by the Riemann method [26]. The Riemann function for Eq. (27) is as follows:

$$q(\phi,\psi;\phi_0,\psi_0)=\exp\left(\frac{\lambda}{2a}(\phi-\phi_0+\psi_0-\psi)\right)\times I_0\left(\frac{\lambda}{a}\sqrt{(\phi-\phi_0)(\psi_0-\psi)}\right) \tag{30}$$

where $I_\nu(z)$ is the modified Bessel function of the first kind with order ν. We obtain the solution $p_\pm(\phi,\psi)$ through Riemann's formula. After change of variables back to z and τ, $p_+(z,\tau)$ and $p_-(z,\tau)$ can be expressed as follows:

$$p_+(z,\tau)=e^{-\lambda\tau}\delta(z-a\tau)+\frac{\lambda}{2a}e^{-\lambda\tau}\sqrt{\frac{a\tau+z}{a\tau-z}}I_1\left(\frac{\lambda}{a}\sqrt{a^2\tau^2-z^2}\right)\times[\theta(z+a\tau)-\theta(z-a\tau)], \tag{31}$$

$$p_-(z,\tau)=\frac{\lambda}{2a}e^{-\lambda\tau}I_0\left(\frac{\lambda}{a}\sqrt{a^2\tau^2-z^2}\right)[\theta(z+a\tau)-\theta(z-a\tau)], \tag{32}$$

where $\theta(z)$ is the Heaviside unit step function. Further discussion of the properties of Eq. (25), which is known as the telegraph equation, can be found in Ref. [27].

We are now in a position to obtain the conditional probability $p(\Delta X=z|\xi(0),\xi(\Delta t))$ from the solution $p_\pm(z,\Delta t)$ in Eqs. (31) and (32). Note that $p_\pm(z,\Delta t)$ satisfy the following normalization condition:

$$\int_{-\infty}^{\infty}p_\pm(z,\Delta t)dz=\frac{1}{2}(1\pm e^{-2\lambda\Delta t})\equiv P_\pm(\Delta t), \tag{33}$$

where $P_+(\Delta t)$ and $P_-(\Delta t)$ are those defined in Eq. (7). Let us define the conditional probability density functions $p_1(z|\Delta t)$ and $p_2(z|\Delta t)$ as follows [see Fig. 2 for the profiles of $p_1(z|\Delta t)$ and $p_2(z|\Delta t)$]:

$$p_1(z|\Delta t) = \frac{p_+(z,\Delta t)}{P_+(\Delta t)},$$

$$p_2(z|\Delta t) = \frac{p_-(z,\Delta t)}{P_-(\Delta t)}. \tag{34}$$

The conditional probability $p(\Delta X = z|\xi(0),\xi(\Delta t))$ is given as follows:

$$p_1(z|\Delta t) \quad \text{if } \xi(0) = \xi(\Delta t) = +a,$$

$$p_1(-z|\Delta t) \quad \text{if } \xi(0) = \xi(\Delta t) = -a,$$

$$p_2(z|\Delta t) \quad \text{if } \xi(0) = +a, \quad \xi(\Delta t) = -a,$$

$$p_2(-z|\Delta t) \quad \text{if } \xi(0) = -a, \quad \xi(\Delta t) = +a. \tag{35}$$

In practical calculations, we apply the following rule to calculate the random increment ΔX. Let us consider the random variables ΔX_1 and ΔX_2 whose probability distributions are governed by $p_1(z|\Delta t)$ and $p_2(z|\Delta t)$, respectively. Then, the probability distribution of the random increment ΔX follows that of one among the following four random variables:

$$\Delta X = \begin{cases} \Delta X_1 & \text{if } \xi(0) = \xi(\Delta t) = +a, \\ -\Delta X_1 & \text{if } \xi(0) = \xi(\Delta t) = -a, \\ \Delta X_2 & \text{if } \xi(0) = +a,\ \xi(\Delta t) = -a, \\ -\Delta X_2 & \text{if } \xi(0) = -a,\ \xi(\Delta t) = +a. \end{cases} \tag{36}$$

The random numbers ΔX_1 and ΔX_2 can be straightforwardly generated using either the inverse transform method or the acceptance-rejection method [28]. Once these ΔX_1 and ΔX_2 have been generated, numerical integration of the trajectory can be pursued by use of Eq. (19). (We call this method A.)

The numerical procedure for method A can be summarized as follows. Given an initial x_0 and $\xi(0)$, we first choose the state of $\xi(\Delta t)$ using the rule shown in Eq. (8). Next, we determine the value of ΔX following the rule shown in Eq. (36). Integration of the trajectory is then performed using Eq. (19).

To check if method A shows the correct limiting behavior for Gaussian white noise, we take the limit $a \to \infty$ and $\lambda \to \infty$ with $a^2/\lambda = 2D$ fixed. Then both $p_1(z|\Delta t)$ and $p_2(z|\Delta t)$ approach the probability distribution of the standard Wiener process which corresponds to the Gaussian distribution

$$\frac{1}{2\sqrt{\pi D \Delta t}} \exp\left(-\frac{z^2}{4D\Delta t}\right). \tag{37}$$

Therefore, the probability distributions of the four cases in Eq. (36) become the same in the Gaussian white noise limit, indicating that the dependence of ΔX on $\xi(0)$ and $\xi(\Delta t)$ disappears in this limit and that the process ΔX becomes Markovian.

The important step in this scheme is to obtain the probability distribution which governs the extended Markovian process $(\xi(\tau), X(\tau))$. Hence method A can be extended, in principle, to any arbitrary type of stochastic process provided the external noise is Markovian. Moreover, the probability distribution of the short time increment of the driving process must be known [see Eq. (12)].

B. Simplified weak Taylor scheme

Since the properties we are interested in are mainly statistical properties obtained by averaging over an ensemble of sample trajectories, the appropriate notion of convergence is usually weak convergence. In this case, it is better to use a simpler numerical scheme in which the original random increment defined in Eq. (12) is replaced by a more easily generated noise increment that still satisfies the same moment properties up to a specified order. For instance, it has been shown that instead of Gaussian increments, much simpler two-point-distributed random variables with similar moment properties can be employed in the Euler scheme [1]. In general, the requirement of the simplified scheme is that the moments of the simplified random variables must coincide with the moments of the original random increments up to a specified order. The procedure based on this idea can be summarized as follows. The random increments ΔX_1 and ΔX_2 in Eq. (36) are replaced by the following two-point-distributed random variables $\Delta\tilde{X}_1$ and $\Delta\tilde{X}_2$, respectively, which have the same moments up to third order as those of ΔX_1 and ΔX_2:

$$\Delta\tilde{X}_i = \begin{cases} R_i & \text{w.p. } q_i \\ L_i & \text{w.p. } 1-q_i \end{cases} \quad (i = 1,2). \tag{38}$$

The values of parameters L_i, R_i, and q_i $(i=1,2)$ are determined as follows.

The nth moment of ΔX_i $(i=1,2)$, defined as

$$\langle \Delta X_i^n \rangle = \int_{-\infty}^{\infty} z^n p_i(z|\Delta t)\, dz, \tag{39}$$

can be calculated using Eqs. (31)–(34) through series expansion of the integrand and term-by-term integration. The moments of ΔX_1 and ΔX_2 up to third order are as follows:

$$\langle \Delta X_1 \rangle = \frac{a}{\lambda} \tanh \lambda \Delta t,$$

$$\langle \Delta X_1^2 \rangle = \frac{a^2 t}{\lambda} \tanh \lambda \Delta t,$$

$$\langle \Delta X_1^3 \rangle = \frac{3a^3}{\lambda^3}(\lambda \Delta t - \tanh \lambda \Delta t), \tag{40}$$

$$\langle \Delta X_2 \rangle = 0,$$

$$\langle \Delta X_2^2 \rangle = \frac{a^2}{\lambda^2}(\lambda \Delta t \coth \lambda \Delta t - 1),$$

$$\langle \Delta X_2^3 \rangle = 0. \tag{41}$$

From the requirement that ΔX_i and $\Delta\tilde{X}_i$ have the same moments up to third order, the values of the parameters govern-

ing the random variables $\Delta\tilde{X}_i$ are determined as follows:

$$R_i = \langle \Delta X_i \rangle + \sqrt{\frac{1-q_i}{q_i}} V_i,$$

$$L_i = \langle \Delta X_i \rangle - \sqrt{\frac{q_i}{1-q_i}} V_i,$$

$$q_i = \frac{1}{2}\left(1 - \frac{A_i}{\sqrt{A_i^2 + 4V_i^3}}\right), \tag{42}$$

where

$$V_i = \langle \Delta X_i^2 \rangle - \langle \Delta X_i \rangle^2,$$

$$A_i = \langle \Delta X_i^3 \rangle - 3\langle \Delta X_i \rangle \langle \Delta X_i^2 \rangle + 2\langle \Delta X_i \rangle^3. \tag{43}$$

The two graphs in Fig. 2 show the characteristic features of the probability distributions of $\Delta\tilde{X}_1$ and $\Delta\tilde{X}_2$. The asymmetric structure of the probability distribution of ΔX_1 is reflected in the distribution of $\Delta\tilde{X}_1$. Since for the case of $p_1(z|\Delta t)$ it is required that the initial state $\xi(0)$ and the final state $\xi(\Delta t)$ have the same state $+a$, the probability of the noise staying in the $+a$ state is higher than that of the noise staying in the $-a$ state, and this is reflected in the probability distribution of $\Delta\tilde{X}_1$. On the other hand, the probability distributions of both ΔX_2 and $\Delta\tilde{X}_2$ are symmetric. Since for $p_2(z|\Delta t)$ it is required that the initial state and the final state be different, there is no preference between the two possible values of $\Delta\tilde{X}_2$. Also, from Eqs. (41) and (42), we know that $q_2 = \frac{1}{2}$ and two possible values of $\Delta\tilde{X}_2$ (L_2 and R_2) are simply expressed as $-\langle \Delta X_2^2 \rangle^{1/2}$ and $\langle \Delta X_2^2 \rangle^{1/2}$.

The dependence of L_i, R_i, and q_i on the integration time step Δt is as follows. In the case of $\Delta\tilde{X}_1$, q_1 decreases from 1 to $\frac{1}{2}$ as Δt increases. When $\lambda\Delta t \ll 1$, $L_1 \sim -\frac{1}{5}a\Delta t$ and $R_1 \sim a\Delta t$, and when $\lambda\Delta t \gg 1$, $L_1 \sim -a\sqrt{\Delta t/\lambda}$ and $R_1 \sim a\sqrt{\Delta t/\lambda}$. On the other hand, in the case of $\Delta\tilde{X}_2$, q_2 is a constant. When $\lambda\Delta t \ll 1$, $L_2 \sim -a\Delta t/\sqrt{3}$ and $R_2 \sim a\Delta t/\sqrt{3}$, and when $\lambda\Delta t \gg 1$, $L_2 \sim -a\sqrt{\Delta t/\lambda}$ and $R_2 \sim a\sqrt{\Delta t/\lambda}$. In the limit of large Δt, the behavior of L_1 and R_1 is similar to that of L_2 and R_2, since the dependence on the previous state diminishes as Δt becomes larger.

Next, we examine the asymptotic behavior of the two-point-distributed random variables $\Delta\tilde{X}_i$ in the Gaussian white noise limit. By taking $a \to \infty$ and $\lambda \to \infty$ with $a^2/\lambda = 2D$ fixed, both $\langle \Delta X_i \rangle$ and $\langle \Delta X_i^3 \rangle$ go to zero and $\langle \Delta X_i^2 \rangle$ approaches $2D\Delta t$. In this limit, both $\Delta\tilde{X}_1$ and $\Delta\tilde{X}_2$ become two-point-distributed random variables having either $+\sqrt{2D\Delta t}$ or $-\sqrt{2D\Delta t}$ with equal probability $\frac{1}{2}$. Therefore if we use Eq. (11) with noise increment $\Delta\tilde{X}_i$, we can recover the simplified weak Euler scheme.

The procedure for the numerical simulation using the simplified random increment $\Delta\tilde{X}_i$ follows the procedure of method A, i.e., we first choose the value of $\xi(\Delta t)$, and then determine the value of ΔX from it. However, since only finite sets of $(\xi(\Delta t), \Delta X)$ are possible in the simplified scheme, those finite sets can be listed explicitly. Depending on the state of $\xi(0)$, the finite sets are

$$(\xi(\Delta t), \Delta X) = \begin{cases} (+a, R_1) & \text{w.p. } q_1 P_+, \\ (+a, L_1) & \text{w.p. } (1-q_1) P_+, \\ (-a, R_2) & \text{w.p. } q_2 P_-, \\ (-a, L_2) & \text{w.p. } (1-q_2) P_- \end{cases} \tag{44}$$

for $\xi(0) = +a$, and

$$(\xi(\Delta t), \Delta X) = \begin{cases} (-a, -R_1) & \text{w.p. } q_1 P_+, \\ (-a, -L_1) & \text{w.p. } (1-q_1) P_+, \\ (+a, -R_2) & \text{w.p. } q_2 P_-, \\ (+a, -L_2) & \text{w.p. } (1-q_2) P_- \end{cases} \tag{45}$$

for $\xi(0) = -a$, where $P_\pm = P_\pm(\Delta t)$. Hence we can obtain $\xi(\Delta t)$ and ΔX using the same procedure. Furthermore, both $\xi(\Delta t)$ and ΔX can be obtained simultaneously from a single use of a random number generator with a uniform distribution.

The procedure of the simplified numerical simulation scheme can be summarized as follows. (We call this method B.) For a given initial x_0 and $\xi(0)$, we obtain $\xi(\Delta t)$ and ΔX according to either (44) or (45) depending on the state of $\xi(0)$. Then x is integrated using Eq. (19). Notice that method A requires the generation of two random numbers: one from a random number generator with uniform distribution for the determination of the state of $\xi(\Delta t)$; and a second one that satisfies either probability distribution p_1 or p_2 depending on the state of $\xi(\Delta t)$, for the determination of the value of ΔX at each integration step. By contrast, method B requires the use of a single random number generator with uniform distribution at each integration step. Generation of a random number satisfying a specified probability distribution generally takes longer than generation of a random number satisfying a uniform distribution. Therefore the computation time required for the simplified scheme (method B) is expected to be much less than that required for the original scheme (method A). Although the parameters R_i, L_i, and q_i have somewhat complicated forms and evaluation of these parameters will take a certain amount of computation time, the values of these parameters are only computed a single time, before the numerical integration loop starts.

IV. NUMERICAL RESULTS AND DISCUSSION

To examine the accuracy of the present numerical methods (methods A and B), we performed numerical simulations of two kinds of typical stochastic differential equations subject to dichotomous noise. The first system considered is a damped free Brownian particle, which is in the form of a linear Langevin equation and thus has plenty of analytical features available. We computed the time-dependent probability distribution, stationary probability distributions, and several moments. In the second example, we consider the mean first-passage time (MFPT) problem in a bistable potential. All of the properties that we obtained numerically have analytical expressions, enabling quantitative assessment of our methods. Since each analytical result found in the litera-

ture was written in its own notation, here we use a standardized notation to present these results in simple forms that are appropriate for our purposes.

A. Damped free Brownian motion

Damped free Brownian motion subject to dichotomous noise is described by the following linear Langevin equation of the velocity of particle $v(t)$:

$$\dot{v}(t) = -\gamma v(t) + \xi(t), \tag{46}$$

where γ is the damping constant and $\xi(t)$ is the dichotomous Markov noise defined in Sec. II. Equation (46) can be considered as describing a particle undergoing Brownian motion under a harmonically bound potential without inertial effects, or describing the output of a low-pass *RC* filter [29,30].

The stationary probability distribution $P_{\mathrm{st}}(v)$ was first obtained by Wonham and Fuller [29] (see also Refs. [18,25,31–33]). $P_{\mathrm{st}}(v)$ has the following form:

$$P_{\mathrm{st}}(v) = \frac{\gamma\Gamma(\lambda/\gamma + 1/2)}{a\sqrt{\pi}\Gamma(\lambda/\gamma)}\left(1 - \frac{\gamma^2 v^2}{a^2}\right)^{\lambda/\gamma - 1} \tag{47}$$

if $-a/\gamma \leqslant v \leqslant a/\gamma$ and is zero otherwise. Equation (47) describes a nonequilibrium phase transition induced by the color of the noise. That is, the distribution P_{st} is either convex or concave depending on the value of the rate λ/γ.

Analytical expressions for the time-dependent probability density $P(v,t)$ can be found in Refs. [18,34,35]. When the initial velocity of the particle is set to zero, that is, for the initial condition $P(v,0) = \delta(v)$, $P(v,t)$ has the following form:

$$P(v,t) = \frac{1}{2}e^{-\lambda t}[\delta(v - v_+(t)) + \delta(v - v_-(t))] + p(v,t)[\theta(v - v_-(t)) - \theta(v - v_+(t))] \tag{48}$$

where $p(v,t)$ is defined in Eq. (49). As a natural consequence of the finite acceleration (either $+a$ or $-a$), $P(v,t)$ has finite support with the boundaries $v_\pm(t) = \pm(1 - e^{-\gamma t})a/\gamma$, and is surrounded by two δ functions. If $v_-(t) < v < v_+(t)$, $P(v,t)$ becomes $p(v,t)$, which has the following form:

$$p(v,t) = \frac{\gamma}{2a}(1 - 2c)\left(\frac{4a^2}{B_+B_-}\right)^c {}_2F_1(c,c;1;\sigma) + \frac{c\gamma}{4a}\left(\frac{4a^2}{B_+B_-}\right)^{c+1} e^{-\gamma t}(1 + e^{\gamma t})\, {}_2F_1(c,c;1;\sigma) + \frac{\gamma}{4a}\left(\frac{4a^2}{B_+B_-}\right)^{c+1} e^{-\gamma t}\left(\frac{A_+}{B_+} + \frac{A_-}{B_-}\right) {}_2F_1'(c,c;1;\sigma) \tag{49}$$

where $c = 1 - \lambda/\gamma$, $A_\pm = a(1 - e^{-\gamma t}) \pm \gamma v$, $B_\pm = a(1 + e^{-\gamma t}) \pm \gamma v$, $\sigma = A_+A_-/B_+B_-$, and ${}_2F_1(c,c;1;\sigma)$ and ${}_2F_1'(c,c;1;\sigma)$ are the hypergeometric function and its derivative with respect to σ, respectively.

By generating a large number of sample trajectories using method A, we obtained the probability density and compared it with the analytical result. For fixed $\gamma = D = 1$ and $a = \sqrt{2D\lambda}$, the numerical results were evaluated for various values of λ ranging from 10^{-1} to 10^3. The integration time step Δt was set to 0.01. Stationary probability distributions were obtained as described in Sec. II and compared with Eq. (47). For the whole range of λ, the numerical results show satisfactory agreement with the analytical results (see Fig. 1). In addition, the results clearly show the phase transition that occurs as the value of λ is varied. The profile of the time-dependent probability density was obtained at $t = 1$ and compared with Eq. (48). The hypergeometric function in Eq. (49) is reduced to the following closed form of σ if λ/γ is a positive integer:

$${}_2F_1(c,c;1;\sigma) = (1 - \sigma)^{-c} P_{-c}\left(\frac{1 + \sigma}{1 - \sigma}\right) \tag{50}$$

where $P_n(z)$ is the Legendre polynomial of z. In this case, the value of $p(v,t)$ can be evaluated explicitly. A total of 10^6 sample trajectories were generated to obtain the probability distribution. The time-dependent probability distribution also shows good agreement with the analytical result (see Fig. 3).

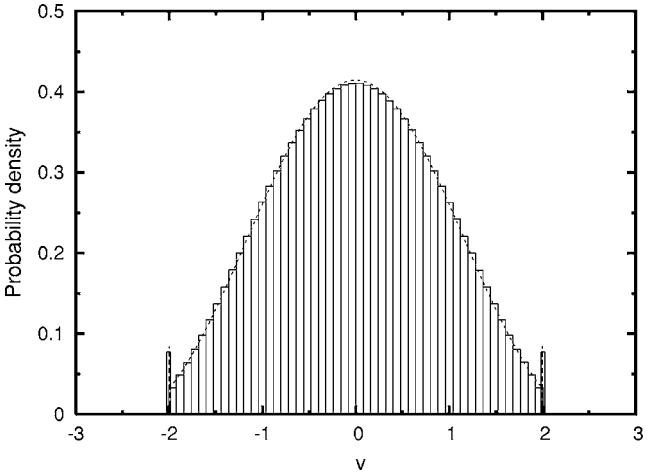

FIG. 3. Time-dependent probability distribution of velocity v obtained from Eq. (46) at $t = 1$ for $\lambda = 5$. The numerical result obtained by method A is presented as a histogram and the analytical result is depicted as a dashed line. The heights of the δ functions are scaled such that the product of the height and the bin size represents the probability of having velocity of the values of the positions of the δ functions.

Although the above results confirm that method A works well for a wide range of λ, there is no clear way to quantitatively estimate the numerical accuracy of the probability density. Instead, we examine the accuracy of the moments $\langle v^n(t)\rangle$. We can obtain the analytical expression for $\langle v^n(t)\rangle$ from the kth correlation ($k \leqslant n$) of the noise $m_k = \langle \xi(t_1)\xi(t_2)\cdots\xi(t_k)\rangle$ for the sequence of time $t_1 \geqslant t_2 \geqslant \cdots \geqslant t_k$. Using Eqs. (2) and (3), we obtain

$$m_{2k} = a^2 e^{-2\lambda(t_1 - t_2)} m_{2k-2},$$

$$m_{2k-1} = 0. \tag{51}$$

The analytical expression of $\langle v^n(t)\rangle$ as well as the characteristic function of the time-dependent probability distribution $P(v,t)$ were presented in Ref. [25].

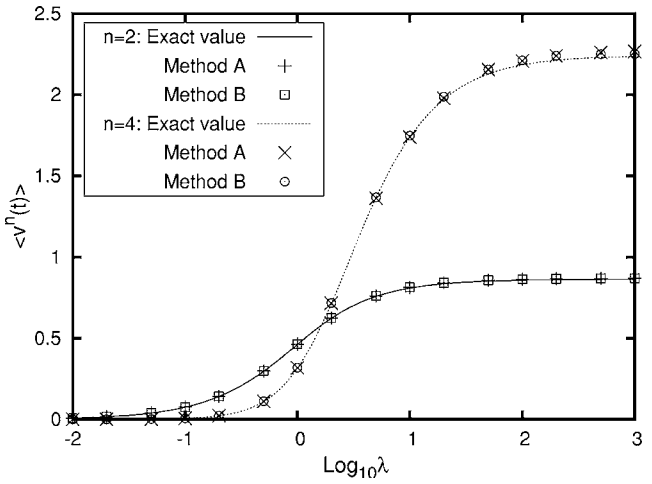

FIG. 4. Plots of the numerical and analytical results for the second moment $\langle v^2(t)\rangle$ and the fourth moment $\langle v^4(t)\rangle$ at $t=1$. The solid and dashed lines represent the analytical $\langle v^2(t)\rangle$ and $\langle v^4(t)\rangle$, respectively. The numerical results for $\langle v^2(t)\rangle$ and $\langle v^4(t)\rangle$ obtained using method A are plotted as open squares and circles, respectively. The numerical results for $\langle v^2(t)\rangle$ and $\langle v^4(t)\rangle$ obtained using method B are plotted + and ×, respectively. The sizes of the error bars for both quantities are smaller than the symbol size. For comparison of the speeds of these methods we refer to Fig. 5.

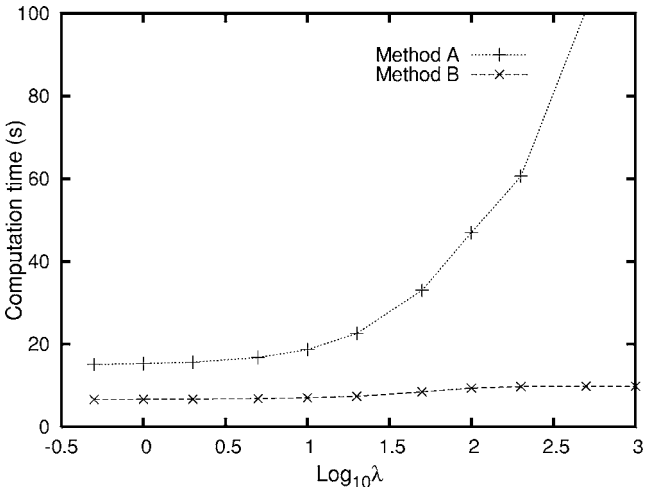

FIG. 5. Comparison of the computation times required for the generation of 10^6 trajectories by methods A and B. Each trajectory is generated on the time interval [0,1] with step size $\Delta t=0.01$. Throughout the calculations, we set $\gamma=D=1$ and $a=\sqrt{2D\lambda}$.

We calculated the second and fourth moments at $t=1$ using methods A and B. Throughout the calculations, $\gamma=D=1$ and $a=\sqrt{2D\lambda}$, and λ varied from 10^{-2} to 10^3. The integration time step Δt was set to 0.01. A total of 10^8 sample trajectories were generated for the calculation of the moments. The moments obtained using methods A and B are presented along with the analytical results in Fig. 4. Both method A and method B provide reasonably accurate numerical results over a wide range of λ, including the region of large λ where the behavior of dichotomous noise approaches that of Gaussian white noise. However, the computation times for method B are markedly lower than the corresponding times for method A. Moreover, this difference increases with increasing λ because the acceptance-rejection method represents a time-consuming step depending on the magnitude of the rate λ. In contrast, method B does not depend on λ (see Fig. 5).

B. Mean first passage time in a bistable potential

Next we consider a bistable system driven by dichotomous noise in an overdamped region, which is described by the following evolution equation:

$$\dot{x}(t) = f(x(t)) + \xi(t), \tag{52}$$

where the drift term is given by $f(x)=-V'(x)=x-x^3$, and $\xi(t)$ is the dichotomous Markov noise defined in Sec. II. The bistable potential $V(x)=-\frac{1}{2}x^2+\frac{1}{4}x^4$ has two minima, at $x=\pm 1$ (stable points), and one maximum, at $x=0$ (unstable point). One of the interesting problems in a bistable system is the mean first-passage time T_{bot} from one minimum $x=-1$ to the other minimum $x=+1$. Balakrishnan *et al.* obtained analytical exprssions for the MFPT and the rate in terms of the stationary probability density [36] which were confirmed by Porrà *et al.* who used a stochastic trajectory analysis [37]. Because $f(x)$ is an odd function, the formal expression for T_{bot} can be reduced to a product of two single integral forms, which is a more convenient for numerical evaluation. Let χ be a real root of the equation $f(\chi)+a=0$. [Transitions from the bottom of one well to the bottom of the other one occur only if $a>2/3\sqrt{3}$, and in this case, the equation $f(\chi)+a=0$ has only one real root.] Then T_{bot} can be expressed as follows:

$$\begin{aligned} T_{\text{bot}} = {} & 4a^2\lambda \int_0^1 q_+(x)q_-(x)e^{-\Phi(x)}dx \int_0^{\chi} q_+(x)q_-(x)e^{\Phi(x)}dx \\ & + 2ae^{-\Phi(1)} \int_0^1 q_+(x)q_-(x)e^{\Phi(x)}dx \\ & + e^{-\Phi(-1)} \int_{-\chi}^{-1} q_+(x)e^{\Phi(x)}dx + \frac{1}{2\lambda} \end{aligned} \tag{53}$$

where

$$q_{\pm} = \frac{1}{a \pm f(x)}, \tag{54}$$

$$\Phi(x) = 2\lambda \int_0^x \frac{f(y)}{a^2 - f^2(y)}dy. \tag{55}$$

The exponential factor $\exp[\Phi(x)]$ in Eq. (53) can be written in a closed form [38]:

$$\begin{aligned} e^{\Phi(x)} = {} & \frac{(\chi^2 - x^2)^{\lambda\alpha} \exp\{-(3\chi/2\beta)\lambda\alpha[\varphi(x+\chi/2) - \varphi(x-\chi/2)]\}}{[(x+\chi/2)^2 + \beta^2]^{\lambda\alpha/2}[(x-\chi/2)^2 + \beta^2]^{\lambda\alpha/2}} \end{aligned} \tag{56}$$

where

TABLE I. Comparison of T_{bot} values obtained by our methods and those obtained by Eq. (53).

		MFPT		
D	λ	Exact value	Method A	Method B
1	1	6.529	6.548±0.008	6.541±0.008
	10	4.160	4.163±0.003	4.163±0.004
	100	3.671	3.735±0.004	3.726±0.003
0.1	10	78.43	79.28±0.06	79.00±0.06
	100	67.51	67.51±0.05	67.48±0.07

$$\alpha = \frac{1}{3\chi^2 - 1}, \quad \beta = \frac{\sqrt{3\chi^2 - 4}}{2}, \tag{57}$$

$$\varphi(x) = \arctan(\beta^{-1} x). \tag{58}$$

We computed the values of T_{bot} by methods A and B for several sets of (D,λ), and compared them with the T_{bot} values obtained using Eq. (53). The integration time step Δt was set to 0.01, and 10^7 sample trajectories were used for the evaluation of T_{bot}. As shown in Table I, the numerical results obtained using methods A and B show good agreement with the exact values over a wide range of λ. It is worth noting that the results obtained using method B show essentially the same level of accuracy as those obtained using method A, even though the computation time for the former method is much lower.

A further increase of the numerical accuracy of the proposed algorithm for the mean first passage time can be expected at fixed step size if a modified conditional probability $p(\Delta X | \xi(0), \xi(\Delta t))$ is used that allows for an absorbing boundary at the final state $x=1$ [39]. So far a proper numerical implementation of absorbing boundary conditions has been achieved only for Gaussian white noise [40].

V. CONCLUSION

In this paper, we have presented a numerical integration scheme for the simulation of stochastic differential equations with dichotomous noise. We used a stochastic Taylor expansion based on the time discretization approximation to derive Eq. (19); hence the numerical scheme maintains first order convergence with respect to the integration time step even in the vicinity of the Gaussian white noise limit. In this approximation, the random increment ΔX, which corresponds to the noise accumulated during the integration time step [see Eq. (12)], depends on the initial and final states of the noise, contrary to the case of Gaussian white noise. Still this process is Markovian in the extended space state (X,ξ). Its probability distribution was obtained from the solution of the master equation (22). The time integration of the sample trajectory proceeds by first choosing the noise state and then determining the value of ΔX by the acceptance-rejection method. The sample trajectory is then updated using Eq. (19).

We also presented a simplified scheme that uses two-point-distributed random variables which satisfy the same moment properties up to the third order instead of the random increment ΔX. In this simplified scheme, the state of the noise and the value of the random increment can be determined simultaneously through a single execution of a random number generator with uniform distribution at each integration step. As a result, the simplified scheme is much more efficient for calculating statistically averaged properties of a system. We applied our two numerical methods (methods A and B) to two prototypical model systems: a damped free Brownian particle, and a Brownian particle in a bistable potential. Both methods produced highly accurate numerical results over a wide range of the noise correlation time, including the regime close to the Gaussian white limit. Moreover the numerical simulations using method B had much shorter computation times.

Finally, we would note that our numerical methods can be applied to systems driven by more general kinds of external noise provided the behavior of the external noise in addition to the random increment defined in Eq. (12) can be described as a Markov process.

ACKNOWLEDGMENT

This work was supported by the Korea Research Foundation Grant No. KRF-2005-070-C00065.

[1] P. E. Kloeden and E. Platen, *Numerical Solution of Stochastic Differential Equations* (Springer-Verlag, Berlin, 1999).
[2] C. W. Gardiner, *Handbook of Stochastic Methods* (Springer-Verlag, Berlin, 1983).
[3] P. Hänggi and H. Thomas, Phys. Rep. **88**, 207 (1982).
[4] H. Risken, *The Fokker Planck Equation* (Springer-Verlag, Berlin, 1984).
[5] P. Hänggi, F. Marchesoni, and P. Grigolini, Z. Phys. B: Condens. Matter **56**, 333 (1984).
[6] P. Hänggi and P. Jung, Adv. Chem. Phys. **89**, 239 (1995); P. Hänggi, Z. Phys. B **31**, 407 (1978).
[7] P. Jung, in *Stochastic Dynamics*, edited by L. Schimansky-Geier and T. Pöschel (Springer-Verlag, Berlin, 1997).
[8] V. Balakrishnan and C. Van den Broeck, Phys. Rev. E **65**, 012101 (2001).
[9] G. N. Milstein, *Numerical Integration of Stochastic Differential Equations* (Ural University Press, Sverdlovsk, 1988) (in Russian), *Mathematics and Its Applications*, Vol. 313 (Kluwer Academic, Dordrecht, 1995).
[10] R. Mannella, in *Noise in Nonlinear Dynamical Systems*, edited by F. Moss and P. V. E. McClintock (Cambridge University Press, Cambridge, U.K., 1989), Vol. 3.
[11] J. M. Sancho, M. San Miguel, S. L. Katz, and J. D. Gunton, Phys. Rev. A **26**, 1589 (1982).

[12] R. F. Fox, Phys. Rev. A **43**, 2649 (1991); R. Mannella and V. Palleschi, *ibid.* **40**, 3381 (1989); R. L. Honeycutt, *ibid.* **45**, 604 (1992); G. N. Milshtein and M. V. Tret'yakov, J. Stat. Phys. **77**, 691 (1994); J. Bao, Y. Abe, and Y. Zhuo, *ibid.* **90**, 1037 (1998).
[13] V. I. Klyatskin, Radiofiz. **20**, 562 (1977) [Radiophys. Quantum Electron. **20**, 382 (1978)].
[14] K. Kitahara, W. Horsthemke, and R. Lefever, Phys. Lett. **70A**, 377 (1979).
[15] P. Hänggi and P. Riseborough, Phys. Rev. A **27**, 3379 (1983).
[16] W. Horsthemke and R. Lefever, *Noise-Induced Transitions* (Springer-Verlag, Berlin, 1984).
[17] C. Van den Broeck and P. Hänggi, Phys. Rev. A **30**, 2730 (1984).
[18] J. M. Sancho, J. Math. Phys. **25**, 354 (1984).
[19] J. Masoliver and J. M. Porrà, Phys. Rev. E **48**, 4309 (1993).
[20] R. F. Pawula, Phys. Rev. A **35**, 3102 (1987).
[21] V. Palleschi, Phys. Lett. A **128**, 318 (1988). See also U. Behn, R. Müller, and P. Talkner, Phys. Rev. E **47**, 3970 (1993), and C. Berghaus, A. Hilgers, and J. Schnakenberg, Z. Phys. B: Condens. Matter **100**, 157 (1996).
[22] C. Van den Broeck, J. Stat. Phys. **31**, 467 (1983).
[23] N. G. van Kampen, J. Stat. Phys. **24**, 175 (1981).
[24] V. Balakrishnan and S. Chaturvedi, Physica A **148**, 581 (1988).
[25] A. Morita, Phys. Rev. A **41**, 754 (1990).
[26] N. S. Koshlyakov, M. M. Smirnov, and R. R. Gliner, *Differential Equations of Mathematical Physics* (North-Holland, Amsterdam, 1964).
[27] A. D. Polyanin, *Handbook of Linear Partial Differential Equations for Engineers and Scientists* (Chapman & Hall/CRC, Boca Raton, FL, 2002).
[28] A. M. Law and W. D. Kelton, *Simulation Modeling and Analysis*, 3rd ed. (McGraw-Hill, New York, 2000).
[29] W. M. Wonham and A. T. Fuller, J. Electron. Control **4**, 567 (1958).
[30] R. F. Pawula, Int. J. Control **26**, 629 (1972).
[31] J. Masoliver, Phys. Rev. E **48**, 121 (1993).
[32] M. O. Cáceres, Phys. Rev. E **67**, 016102 (2003).
[33] R. F. Pawula, IEEE Trans. Inf. Theory **13**, 33 (1967).
[34] W. M. Wonham, J. Electron. Control **6**, 376 (1959).
[35] R. F. Pawula, Int. J. Control **12**, 25 (1970).
[36] V. Balakrishnan, C. Van den Broeck, and P. Hänggi, Phys. Rev. A **38**, 4213 (1988).
[37] J. M. Porrà, J. Masoliver, and K. Lindenberg, Phys. Rev. A **44**, 4866 (1991). See also J. M. Porrà, Jaume Masoliver, Katja Lindenberg, Ivan L'Heureux, and Raymond Karpral, *ibid.* **45**, 6092 (1992).
[38] I. L'Heureux and R. Kapral, J. Chem. Phys. **90**, 2453 (1989).
[39] P. Hänggi and P. Talkner, Phys. Rev. A **32**, 1934 (1985).
[40] M. Schindler, P. Talkner, and P. Hänggi, Physica A **351**, 40 (2005).